

# Optimal witnessing of the quantum Fisher information with few measurements

Iagoba Apellaniz,<sup>1</sup> Matthias Kleinmann,<sup>1</sup> Otfried Gühne,<sup>2</sup> and Géza Tóth<sup>1,3,4,\*</sup>

<sup>1</sup>*Department of Theoretical Physics, University of the Basque Country UPV/EHU, E-48080 Bilbao, Spain*

<sup>2</sup>*Naturwissenschaftlich-Technische Fakultät, Universität Siegen, Walter-Flex-Str. 3, 57068 Siegen, Germany*

<sup>3</sup>*IKERBASQUE, Basque Foundation for Science, E-48013 Bilbao, Spain*

<sup>4</sup>*Wigner Research Centre for Physics, Hungarian Academy of Sciences, H-1525 Budapest, Hungary*

(Published: 28 March 2017)

We show how to verify the metrological usefulness of quantum states based on the expectation values of an arbitrarily chosen set of observables. In particular, we estimate the quantum Fisher information as a figure of merit of metrological usefulness. Our approach gives a tight lower bound on the quantum Fisher information for the given incomplete information. We apply our method to the results of various multiparticle quantum states prepared in experiments with photons and trapped ions, as well as to spin-squeezed states and Dicke states realized in cold gases. Our approach can be used for detecting and quantifying metrologically useful entanglement in very large systems, based on a few operator expectation values. We also gain new insights into the difference between metrological useful multipartite entanglement and entanglement in general.

DOI: [10.1103/PhysRevA.95.032330](https://doi.org/10.1103/PhysRevA.95.032330)

## I. INTRODUCTION

Entanglement lies at the heart of many problems in quantum mechanics and has attracted increasing attention in recent years. There are now efficient methods to detect it with a moderate experimental effort [1,2]. However, in spite of intensive research, many of the intriguing properties of entanglement are not fully understood. One such puzzling fact is that, while entanglement is a sought after resource, not all entangled states are useful for some particular quantum information processing task. For instance, it has been realized recently that entanglement is needed in very general metrological tasks to achieve a high precision [3]. Remarkably, this is true even in the case of millions of particles, which is especially important for characterizing the entanglement properties of cold atomic ensembles [4–9]. However, there are highly entangled pure states that are useless for metrology [10].

In the light of these results, besides verifying that a quantum state is entangled, we should also show that it is useful for metrology. This is possible if we know the quantum Fisher information  $\mathcal{F}_Q[\varrho, J_l]$  for the state. Here  $\varrho$  is a density matrix of an ensemble of  $N$  two-level systems (i.e., qubits),  $J_l = \frac{1}{2} \sum_n \sigma_l^{(n)}$  for  $l = x, y, z$  are the angular momentum components and  $\sigma_l^{(n)}$  are the Pauli spin matrices acting on qubit  $n$ .

The quantum Fisher information is a central quantity of quantum metrology. It is connected to the task of estimating the phase  $\theta$  for the unitary dynamics of a linear interferometer  $U = \exp(-iJ_l\theta)$ , assuming that we start from  $\varrho$  as the initial state. It provides a tight bound for the precision of phase estimation as [11,12]

$$(\Delta\theta)^2 \geq 1/\mathcal{F}_Q[\varrho, J_l]. \quad (1)$$

It has been shown that if  $\mathcal{F}_Q[\varrho, J_l]$  is larger than the value achieved by product states [3], then the state  $\varrho$  is entangled.

Higher values of the quantum Fisher information indicate even multipartite entanglement [13]; this fact has been used to analyze the results of several experiments [8,9,14].

In this paper, we suggest estimating the quantum Fisher information based on a few measurements [15]. Our method can be called “witnessing the quantum Fisher information” since our estimation scheme is based on measuring operator expectation values similarly to how entanglement witnesses work [1,2]. Our findings are expected to simplify the experimental determination of metrological sensitivity since the proposed set of a few measurements is much easier to carry out than the direct determination of the metrological sensitivity, which has been applied in several experiments [8,9,16,17]. The archetypical criterion in this regard is [3]

$$\mathcal{F}_Q[\varrho, J_y] \geq \frac{\langle J_z \rangle^2}{(\Delta J_x)^2}, \quad (2)$$

which is expected to work best for states that are almost completely polarized in the  $z$  direction and spin-squeezed in the  $x$  direction. Apart from spin-squeezed states, there are conditions similar to Eq. (2) for symmetric states close to Dicke states [18–21] and for two-mode squeezed states [22].

After finding criteria for various systems, it is crucial to develop a general method that provides an *optimal* lower bound on the quantum Fisher information in a wide class of cases, especially for the states most relevant for experiments such as spin-squeezed states [23], Greenberger-Horne-Zeilinger (GHZ) states [24], and symmetric Dicke states [18]. It seems that such a method would involve a numerical minimization over all density matrix elements constrained for some operator expectation values, which would be impossible except in very small systems.

In this paper, we demonstrate that tight lower bounds on the quantum Fisher information can still be computed efficiently. Remarkably, our method works for thousands of particles. We show how to obtain a bound on the quantum Fisher information from fidelity measurements for GHZ states [25–32] and for symmetric Dicke states [14,33–37]. We also discuss how to obtain such bounds based on collective measurements for spin-squeezed states of thousands of atoms [6,7,38] and for sym-

\* [toth@alumni.nd.edu](mailto:toth@alumni.nd.edu); <http://www.gtoth.eu>

metric Dicke states prepared recently in cold gases [8,39–41]. We stress that the method is very general, and needs only the expectation values of a set of operators chosen by the experimenter. Then it provides a tight lower bound on the quantum Fisher information.

Due to the relation between the quantum Fisher information and entanglement mentioned above, our method can also be used for entanglement detection and quantification based on an arbitrary set of operator expectation values in very large systems. So far, methods that can be used for large systems, such as spin-squeezing inequalities [42–44], work only for a specific set of observables. In addition, methods that can quantify entanglement based on the expectation values of an arbitrary set of observables, such as semidefinite programming [45–47], work only for small systems.

The paper is organized as follows. In Sec. II, we show how to bound the quantum Fisher information based on the knowledge of some operator expectation values. In Sec. III, we test our method on theoretical examples in small systems. In Sec. IV, we present calculations for experimental data. Finally, in Sec. V, we discuss how the quantum Fisher information is expected to scale with the particle number in the limit of large particle numbers.

## II. ESTIMATION OF THE QUANTUM FISHER INFORMATION

In this section, first we review some important properties of the quantum Fisher information. Then we present our method for estimating it based on a few measurements.

### A. Entanglement quantification with the quantum Fisher information

In Sec. I, we mentioned briefly, how quantum Fisher information connects quantum metrology and entanglement theory. In more detail, the bounds on the quantum Fisher information make it possible to detect metrologically useful entanglement. It has been shown that if

$$\mathcal{F}_Q[\varrho, J_I] > (k-1)N, \quad (3)$$

where  $k$  is an integer, then the state has a better metrological performance than any state with at most  $(k-1)$ -particle entanglement, hence it possesses at least  $k$ -particle metrologically useful entanglement [3,13]. We can immediately see that a perfect  $N$ -particle GHZ state possesses metrologically useful  $N$ -particle entanglement. Based on the ideas above, it is possible to use the quantum Fisher information for entanglement detection [8,9,14].

Let us analyze the condition, Eq. (3), further. A simple calculation shows that for a tensor product of  $(k-1)$ -particle GHZ states the two sides of Eq. (3) are equal. Hence, a state is detected by Eq. (3) if it performs better than a state in which all particles are in GHZ states of  $(k-1)$  particles. For instance, if in an experiment with 10 000 particles we detect five-particle metrologically useful entanglement, then the state is better

metrologically than a tensor product of 2500 four-particle GHZ states. Based on this example, it is easy to see that the requirements for metrologically useful  $k$ -particle entanglement are much stricter than for general  $k$ -particle entanglement.

### B. Estimation of a general function of $\varrho$

First, we review a method that can be used to find a lower bound on a convex function  $g(\varrho)$  based on only a single operator expectation value  $w = \langle W \rangle_\varrho = \text{Tr}(W\varrho)$ . Theory tells us that a tight lower bound can be obtained as [48–50]

$$g(\varrho) \geq \mathcal{B}(w) := \sup_r [rw - \hat{g}(rW)], \quad (4)$$

where  $\hat{g}$  is the Legendre transform, in this context defined as

$$\hat{g}(W) = \sup_{\varrho} [\langle W \rangle_\varrho - g(\varrho)]. \quad (5)$$

Equation (4) has been applied to entanglement measures [49,50]. Since those are defined as convex roofs over all possible decompositions of the density matrix, it is sufficient to carry out the optimization in Eq. (4) for pure states only. However, still an optimization over a general pure state, i.e., over many variables, has to be carried out, which is practical only for small systems.

Based on this method, we would like to estimate the quantum Fisher information, which is strongly connected to entanglement, while it also has a clear physical meaning in metrological applications. As the first step, we note that  $\mathcal{F}_Q[\varrho, J_I]$  can be obtained as a closed formula with  $\varrho$  and  $J_I$  [12], however, this is a highly nonlinear expression which would make the computation of the Legendre transform very demanding. A key point in our approach is using a very recent finding showing that  $\mathcal{F}_Q[\varrho, J_I]$  is the convex roof of  $4(\Delta J_y)^2$  [51], and hence the optimization may be carried out only for pure states. With this, however, we are still facing an optimization problem that cannot be solved numerically for system sizes relevant for quantum metrology.

We now arrive at our first main result. We show that, for the quantum Fisher information, Eq. (5) can be rewritten as an optimization over a *single* real parameter.

*Observation 1.* The quantum Fisher information can be estimated using the Legendre transform

$$\hat{\mathcal{F}}_Q(W) = \sup_{\mu} \{ \lambda_{\max} [W - 4(J_I - \mu)^2] \}, \quad (6)$$

where  $\lambda_{\max}(A)$  denotes the maximal eigenvalue of  $A$ .

*Proof.* Based on the previous discussion, we can rewrite the right-hand side of Eq. (5) for our case as

$$\hat{\mathcal{F}}_Q(W) = \sup_{\Psi} [\langle W - 4J_I^2 \rangle_{\Psi} + 4 \langle J_I \rangle_{\Psi}^2]. \quad (7)$$

Equation (7) is quadratic in operator expectation values. It can be rewritten as an optimization linear in operator expectation values as

$$\hat{\mathcal{F}}_Q(W) = \sup_{\Psi, \mu} [\langle W - 4J_I^2 \rangle_{\Psi} + 8\mu \langle J_I \rangle_{\Psi} - 4\mu^2], \quad (8)$$

which can be reformulated as Eq. (6). At the extremum, the derivative with respect to  $\mu$  must be 0, hence at the optimum  $\mu = \langle J_I \rangle_\Psi$ . This also means that we have to test  $\mu$  values in the interval  $-N/2 \leq \mu \leq N/2$  only. ■

In this paper, we use Eq. (6) to calculate the Legendre transform [52]. The full optimization problem to be solved consists of Eq. (6) and Eq. (4) with the substitutions  $g(\varrho) = \mathcal{F}_Q[\varrho, J_I]$  and  $\hat{g}(W) = \hat{\mathcal{F}}_Q(W)$ .

We want to stress the generality of our findings beyond the linear interferometers covered in this article. For nonlinear interferometers [53–58], the phase  $\theta$  must be estimated in a unitary dynamics  $U = \exp(-iA\theta)$ , where  $A$  is not a sum of single spin operators and, hence, is different from the angular momentum components. Using Observation 1, we can obtain lower bounds for the corresponding quantum Fisher information  $\mathcal{F}_Q[\varrho, A]$  if we replace  $J_I$  with  $A$  in Eq. (6).

### C. Measuring several observables

We now consider the estimation of the quantum Fisher information based on several expectation values. We can generalize the method described by Eqs. (4) and (5) for measuring several observables  $W_k$  as [49]

$$\mathcal{F}_Q[\varrho, J_y] \geq \sup_{r_1, r_2, \dots, r_K} \left[ \sum_{k=1}^K r_k w_k - \hat{\mathcal{F}}_Q \left( \sum_{k=1}^K r_k W_k \right) \right], \quad (9)$$

where  $w_k = \langle W_k \rangle_\varrho$ . As we can see, we now have several parameters  $r_k$ . Combining Eq. (9) with the Legendre transform (6), we arrive at the formula

$$\mathcal{F}_Q[\varrho, J_I] \geq \sup_{\{r_k\}} \left[ \sum_k r_k w_k - \sup_{\mu} \lambda_{\max}(M) \right], \quad (10)$$

where

$$M = \sum_k r_k W_k - 4(J_I - \mu)^2. \quad (11)$$

Since  $\hat{\mathcal{F}}_Q(\sum r_k W_k)$  is a convex function in  $r_k$ , in Eq. (10) the quantity to be maximized in  $r_k$  is concave [48]. Thus, we can easily find the maximum with the gradient method. If we do not find the optimal  $r_k$ , then we underestimate the real bound. Hence, we will still have a valid lower bound. This does not hold for the optimization over  $\mu$ . The function to be optimized is not a convex function of  $\mu$ , and not finding the optimal  $\mu$  leads to overestimating the bound. Thus, great care must be taken when optimizing over  $\mu$ .

## III. EXAMPLES

In this section, we show how to use our method to estimate the quantum Fisher information based on fidelity measurements, as well as collective measurements.

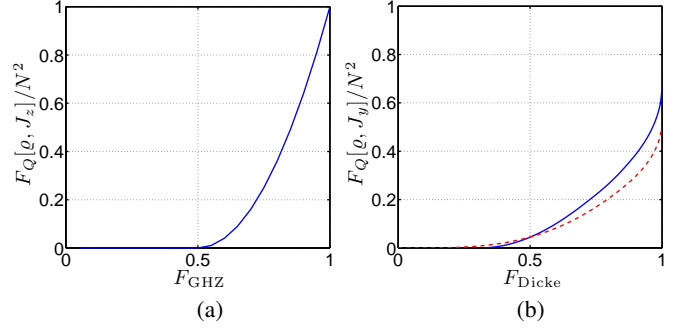


FIG. 1. (a) Fidelity vs. lower bound on the quantum Fisher information for GHZ states of  $N$  qubits. The quantum Fisher information is 0 if the fidelity is less than 0.5. (b) The same, but for Dicke states for with  $N = 6$  (solid line) and  $N = 40$  (dashed line).

### A. Exploiting symmetries

When making calculations for quantum systems with an increasing number of qubits, we soon run into difficulties when computing the largest eigenvalue of Eq. (6). The reason is that for  $N$  qubits, we need to handle  $2^N \times 2^N$  matrices, hence we are limited to systems of 10–15 qubits.

We can obtain bounds for much larger particle numbers, if we restrict ourselves to the symmetric subspace [59]. This approach can give optimal bounds for many systems, such as Bose-Einstein condensates of two-state atoms, which are in a symmetric multiparticle state. The bound computed for the symmetric subspace might not be correct for general states.

Finally, it is important to note that if the operator  $W$  is permutationally invariant and the eigenstate with the maximal eigenvalue of the matrix in Eq. (6) is nondegenerate, then the two bounds coincide, as shown in Appendix B.

### B. Fidelity measurements

Let us examine the case where  $W$  is a projector onto a pure quantum state. First, we consider GHZ states [24]. We choose  $W = |\text{GHZ}\rangle\langle\text{GHZ}|$ , hence  $\langle W \rangle$  is equal to  $F_{\text{GHZ}}$ , the fidelity with respect to the GHZ state. Based on knowing  $F_{\text{GHZ}}$ , we would like to estimate  $\mathcal{F}_Q[\varrho, J_z]$ .

*Observation 2.* A sharp lower bound on the quantum Fisher information with the fidelity  $F_{\text{GHZ}}$  is given by

$$\frac{\mathcal{F}_Q[\varrho, J_z]}{N^2} \geq \begin{cases} (1 - 2F_{\text{GHZ}})^2 & \text{if } F_{\text{GHZ}} > 1/2, \\ 0 & \text{if } F_{\text{GHZ}} \leq 1/2. \end{cases} \quad (12)$$

The proof is based on carrying out the optimization described above analytically and can be found in Appendix A [60]. Equation (12) is plotted in Fig. 1(a). Note that the bound on the quantum Fisher information normalized by  $N^2$  in Eq. (12) is independent of the number of particles. Moreover, the bound is 0 for  $F_{\text{GHZ}} \leq 0.5$ . This is consistent with the fact that for the product state  $|111\dots 11\rangle$  we have  $F_{\text{GHZ}} = 1/2$ , while  $\mathcal{F}_Q[\varrho, J_z] = 0$ .

Next, let us consider symmetric Dicke states. An  $N$ -qubit

symmetric Dicke state is given as

$$|D_N^{(m)}\rangle = \binom{N}{m}^{-\frac{1}{2}} \sum_k \mathcal{P}_k(|1\rangle^{\otimes m} \otimes |0\rangle^{\otimes (N-m)}), \quad (13)$$

where the summation is over all the different permutations of the product state having  $m$  particles in the  $|1\rangle$  state and  $(N-m)$  particles in the  $|0\rangle$  state.

From the point of view of metrology, we are interested mostly in the symmetric Dicke state for even  $N$  and  $m = \frac{N}{2}$ . This state is known to be highly entangled [61,62] and allows for Heisenberg limited interferometry [63]. In the following, we omit the superscript giving the number of  $|1\rangle$ 's and use the notation

$$|D_N\rangle \equiv |D_N^{(\frac{N}{2})}\rangle. \quad (14)$$

The witness operator that can be used for noisy Dicke states is  $W = |D_N\rangle\langle D_N|$ , hence for the expectation value of the witness it is just the fidelity with respect to Dicke states, i.e.,  $\langle W \rangle = F_{\text{Dicke}}$ . In Fig. 1(b), we plot the results for Dicke states of various numbers of qubits. Now the normalized curve is not the same for all particle numbers.  $F_{\text{Dicke}} = 1$  corresponds to  $\mathcal{F}_Q[\varrho, J_y] = N(N+2)/2$ . At this point note that for the examples presented above, the quantum Fisher information scales as  $O(N^2)$  if the quantum state has been prepared perfectly, where  $O(x)$  is the usual Landau notation used to describe the asymptotic behavior of a quantity for large  $x$  [13].

Note that estimating  $\mathcal{F}_Q[\varrho, J_y]$  based on  $F_{\text{Dicke}}$  was possible for 40 qubits in Fig. 1(b), since we carried out the calculations for the symmetric subspace. For our case, the witness operator  $W$  is permutationally invariant and it has a nondegenerate eigenstate corresponding to the maximal eigenvalue. Hence, based on the arguments in Sec. III A the bound is valid even for general, i.e., nonsymmetric states. Further calculations for the large- $N$  limit are given in Appendix C.

### C. Spin-squeezed states

In the case of spin-squeezing, the quantum state has a large spin in the  $z$  direction, but a decreased variance in the  $x$  direction. By measuring  $\langle J_z \rangle$  and  $(\Delta J_x)^2$  we can estimate the quantum Fisher information by Eq. (2). However, this formula does not necessarily give the best lower bound for all values of the collective observables. With our approach we can find the best bound.

To give a concrete example, we choose  $W_1 = J_z$ ,  $W_2 = J_x^2$ , and  $W_3 = J_x$  for the operators to be measured. We change  $w_1$  and  $w_2$  in some interval. We also require that  $w_3 = 0$ , since we assume that the mean spin points in the  $z$  direction [64]. This is reasonable since in most spin-squeezing experiments we know the direction of the mean spin.

Our results are shown in Fig. 2(a). We chose  $N = 4$  particles since for small  $N$  the main features of the plot are clearly visible. The white areas correspond to nonphysical combinations of expectation values. States at the boundary can be obtained as ground states of  $H_{\text{bnd}}^{(\pm)}(\mu) = \pm J_x^2 - \mu J_z$  (Appendix D). In

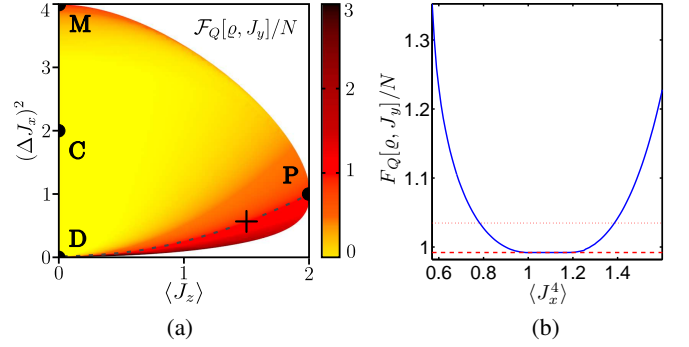


FIG. 2. (a) Optimal lower bound on the quantum Fisher information  $\mathcal{F}_Q[\varrho, J_y]$  based on collective measurements for spin-squeezing with  $N = 4$ . The mean spin points in the  $z$  direction. Below the dashed line we have  $\mathcal{F}_Q[\varrho, J_y]/N > 1$ . For the description of points P, D, M, and C, see the text. (b) Lower bound on  $\mathcal{F}_Q[\varrho, J_y]$  for  $\langle J_z \rangle = 1.5$  and  $(\Delta J_x)^2 = 0.567$ , as a function of  $\langle J_x^4 \rangle$ . The corresponding point in (a) is denoted by a cross. Dashed horizontal line: Lower bound without constraining  $\langle J_x^4 \rangle$ . Dotted horizontal line: Lower bound for states in the symmetric subspace. As shown, an additional constraint or assuming symmetry improves the bound.

Fig. 2(a), the state fully polarized in the  $z$  direction, an initial state for spin-squeezing experiments, corresponds to point P. The Dicke state, (14), corresponds to point D [65]. Spin-squeezing makes  $(\Delta J_x)^2$  decrease, while  $\langle J_z \rangle$  also decreases somewhat. Hence, at least for small squeezing, it corresponds to moving down from point P towards point D on the boundary of the plot, while the metrological usefulness is increasing. Below the dashed line  $\mathcal{F}_Q[\varrho, J_y]/N > 1$ , hence the state possesses metrologically useful entanglement [3]. The equal mixture of  $|000..00\rangle_x$  and  $|111..11\rangle_x$  corresponds to point M, with  $\mathcal{F}_Q[\varrho_M, J_y] = N$ . Finally, the completely mixed state corresponds to point C. It cannot be used for metrology, hence  $\mathcal{F}_Q[\varrho_C, J_y] = 0$ .

We now compare the difference between our bound and Eq. (2). First, we consider the experimentally relevant region for which  $(\Delta J_x)^2 < 1$ . We find that for points that are away from the boundary at least by 0.01 on the vertical axis, the difference between the two bounds for  $\mathcal{F}_Q[\varrho, J_y]$  is smaller than  $2 \times 10^{-6}$ . For points at the boundary the difference is somewhat larger but still small; the relative difference is less than 2% (see Appendix E). Hence, Eq. (2) practically coincides with the optimal bound for  $(\Delta J_x)^2 < 1$ . We now consider the region in Fig. 2(a) for which  $(\Delta J_x)^2 > 1$ . The difference between the two bounds is now larger. It is largest at point M, for which the bound, (2), is 0. Hence, for measurement values corresponding to points close to M, our method could improve formula (2). It is important from the point of view of applying our method to spin-squeezing experiments that the bound, (2), can be substantially improved even for  $(\Delta J_x)^2 < 1$ , if we assume a bosonic symmetry or we measure an additional quantity, such as  $\langle J_x^4 \rangle$  as shown in Fig. 2(b).

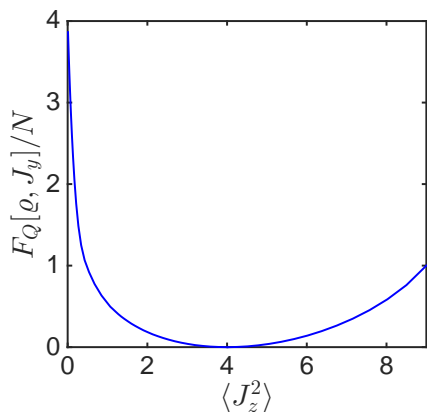


FIG. 3. Optimal lower bound on the quantum Fisher information for symmetric states close to Dicke states for  $N = 6$ .

#### D. Dicke states

In this section, we use our method to find lower bounds on the quantum Fisher information for states close to the Dicke states, (14), based on collective measurements. We discuss what operators have to be measured to estimate the metrological usefulness of the state. In Sec. IV B 2, we test our approach for a realistic system with very many particles.

In order to estimate the metrological usefulness of states created in such experiments, we choose to measure  $W_1 = J_x^2$ ,  $W_2 = J_y^2$ , and  $W_3 = J_z^2$  since the expectation values of these operators uniquely define the ideal Dicke state, and they have already been used for entanglement detection [39]. In cold gas experiments it is common that the state created is invariant under transformations of the type  $U_z(\phi) = \exp(-iJ_z\phi)$  [21]. For such states  $\langle J_x^2 \rangle = \langle J_y^2 \rangle$ , which we also use as a constraint in our optimization.

Let us demonstrate how our method works in an example for small systems. Figure 3 shows the results for  $N = 6$  particles for symmetric states for which

$$\langle J_x^2 + J_y^2 + J_z^2 \rangle = \frac{N}{2} \left( \frac{N}{2} + 1 \right) =: \mathcal{J}_N. \quad (15)$$

It can be seen that the lower bound on the quantum Fisher information is the largest for  $\langle J_z^2 \rangle = 0$ . It reaches the value corresponding to the ideal Dicke state,  $N(N+2)/2 = 24$ . It is remarkable that the state is also useful for metrology if  $\langle J_z^2 \rangle$  is very large. In this case  $\langle J_x^2 \rangle$  and  $\langle J_y^2 \rangle$  are smaller than  $\langle J_z^2 \rangle$ , and this cigar-shaped uncertainty ellipse can be used for metrology.

### IV. CALCULATIONS FOR EXPERIMENTAL DATA

In this section, we use our method to find tight lower bounds on the quantum Fisher information based on experimental data. First, we determine the quantum Fisher information for several experiments in photons and trapped ions creating GHZ states and Dicke states, in which the fidelity has been measured [14,27,29–36,66–68]. Our method is much simpler than obtaining the quantum Fisher information from the density matrix [14] or estimating it from a metrological procedure [8]. Second, we obtain a bound on the quantum Fisher information for

a spin-squeezing experiment with thousands of particles [7]. Based on numerical examples, we see that the bound, (2), is close to optimal even if the state is not completely polarized. Assuming symmetry or knowing additional expectation values can improve the bound (2). Finally, we also obtain the bound for the quantum Fisher information for a recent experiment with Dicke states [39]. The estimate of the precision based on considering the particular case where  $\langle J_z^2 \rangle$  is measured for parameter estimation [21] is close to the optimal bound computed by our method.

#### A. Few-particle experiments

We now estimate the quantum Fisher information based on the fidelity with respect to Dicke states and GHZ states for several experiments with photons and trapped cold ions, following the ideas in Sec. III B.

Our results are summarized in Table I. For the experiments aiming to create Dicke states, the lower bound on  $\mathcal{F}_Q[\varrho, J_y]/N^2$  is shown, while for the experiments with GHZ states we estimate  $\mathcal{F}_Q[\varrho, J_z]/N^2$ . In [29,36] several logical qubits are stored in a particle, but in the rest of the experiments only a single qubit. Reference [32] describes experiments with 2–14 ions, of which we analyze the 8-qubit and 10-qubit GHZ states. Finally, for the experiment in Ref. [66] we used the fidelity estimated using reasonable assumptions discussed in that paper, while the worst-case fidelity is lower.

We can compare our estimate to the quantum Fisher information of the state for the experiment in Ref. [14], where the quantum Fisher information for the density matrix was obtained as  $\mathcal{F}_Q[\varrho, J_y]/N^2 = (10.326 \pm 0.093)/N^2 = (0.6454 \pm 0.0058)$ . As reported in Table I, this value is larger than the one we obtained, however, it was calculated by knowing the entire density matrix, while our bound is obtained from the fidelity alone.

#### B. Many-particle experiments

So far, we have studied the quantum state of few particles. Next we turn to experiments with very many particles, in which a fidelity measurement is not practical. In such systems, the quantum Fisher information must be estimated based on collective measurements.

By far the most relevant quantum states in many-particle experiments are spin-squeezed states, which can be used to increase the precision in magnetometry and in atomic clocks [42]. We also discuss Dicke states, since they have been realized in several experiments [8,39–41]. Dicke states realized in cold gases are the focus of our attention, since they can be used for high-precision interferometry [63].

##### 1. Spin-squeezing experiment

We now use our method to find lower bounds on the quantum Fisher information for a recent spin-squeezing experiment in cold gases, following the ideas in Sec. III C. With it

Physical system	Targeted quantum state		$\frac{\mathcal{F}_Q}{N^2} \geq$	Ref. No.
	Fidelity			
Photons	D <sub>4</sub> ⟩	0.844 ± 0.008	0.358 ± 0.011	[33]
		0.78 ± 0.005	0.281 ± 0.059	[36]
		0.8872 ± 0.0055	0.420 ± 0.009	[14]
		0.873 ± 0.005	0.351 ± 0.006	[69]
Photons	D <sub>6</sub> ⟩	0.654 ± 0.024	0.141 ± 0.019	[34]
		0.56 ± 0.02	0.0761 ± 0.012	[35]
Photons	GHZ <sub>4</sub> ⟩	0.840 ± 0.007	0.462 ± 0.019	[27]
	GHZ <sub>5</sub> ⟩	0.68	0.130	[66]
	GHZ <sub>8</sub> ⟩	0.59 ± 0.02	0.032 ± 0.016	[67]
	GHZ <sub>8</sub> ⟩	0.776 ± 0.006	0.305 ± 0.013	[29]
	GHZ <sub>10</sub> ⟩	0.561 ± 0.019	0.015 ± 0.011	[29]
Trapped ions	GHZ <sub>3</sub> ⟩	0.89 ± 0.03	0.608 ± 0.097	[30]
	GHZ <sub>4</sub> ⟩	0.57 ± 0.02	0.020 ± 0.013	[31]
	GHZ <sub>6</sub> ⟩	≥ 0.509 ± 0.004	0.0003 ± 0.0003	[68]
	GHZ <sub>8</sub> ⟩	0.817 ± 0.004	0.402 ± 0.010	[32]
	GHZ <sub>10</sub> ⟩	0.626 ± 0.006	0.064 ± 0.006	[32]

TABLE I. Fidelity values and the corresponding bounds on the quantum Fisher information for several experiments with Dicke states and GHZ states. For experiments targeting Dicke states, bounds on  $\mathcal{F}_Q[\varrho, J_y]/N^2$  are listed. The maximal value of this quantity is 0.75 and 0.67 for  $N = 4$  and  $N = 6$ , respectively. For experiments with GHZ states, bounds on  $\mathcal{F}_Q[\varrho, J_z]/N^2$  are shown, and, in this case, the maximal value is 1.

we show that the lower bound given in Eq. (2) is close to optimal in this case. We also demonstrate that we can carry out calculations for real systems.

In particular, for our calculations we use the data from the spin-squeezing experiment in Ref. [7]. The particle number is  $N = 2300$ , and the spin-squeezing parameter, defined as

$$\xi_s^2 = N \frac{(\Delta J_x)^2}{\langle J_z \rangle^2}, \quad (16)$$

has the value  $\xi_s^2 = -8.2\text{dB} = 10^{-8.2/10} = 0.1514$ . The spin length  $\langle J_z \rangle$  has been close to maximal. In our calculations, we choose

$$\langle J_z \rangle = \alpha \frac{N}{2}, \quad (17)$$

where we test our method with various values for  $\alpha$ . For each  $\alpha$ , we use a value for  $(\Delta J_x)^2$  such that we get the experimentally obtained spin-squeezing parameter, (16). Moreover, we assume that  $\langle J_x \rangle = 0$ , as the  $z$ -direction was the direction of the mean spin in the experiment. Based on Eq. (2), the bound for the quantum Fisher information is obtained as

$$\frac{\mathcal{F}_Q[\varrho_N, J_y]}{N} \geq \frac{1}{\xi_s^2} = 6.605. \quad (18)$$

where  $\varrho_N$  is the state of the system in the experiment satisfying Eqs. (16) and (17).

We carry out the calculations for symmetric states. This way we obtain a lower bound on the quantum Fisher information, which we denote  $\mathcal{B}_{\text{sym}}(\langle J_z \rangle_{\varrho_N}, \langle J_x^2 \rangle_{\varrho_N})$ . As mentioned in Sec. III B, we could obtain a bound for the quantum Fisher information that is valid even for general, not necessarily symmetric states if the matrix in Eq. (6) had nondegenerate eigenvalues. This is not the case for the spin-squeezing problem. However, we still know that the bound obtained with our calculations restricted to the symmetric subspace cannot be smaller than the optimal bound for general states,  $\mathcal{B}(\langle J_z \rangle_{\varrho_N}, \langle J_x^2 \rangle_{\varrho_N})$ . On the other hand, we know that bound (2) cannot be larger than the optimal bound for general states. These relations can be summarized as

$$\begin{aligned} \mathcal{B}_{\text{sym}}(\langle J_z \rangle_{\varrho_N}, \langle J_x^2 \rangle_{\varrho_N}) &\geq \mathcal{B}(\langle J_z \rangle_{\varrho_N}, \langle J_x^2 \rangle_{\varrho_N}) \\ &\geq \frac{\langle J_z \rangle_{\varrho_N}^2}{(\Delta J_x)_{\varrho_N}^2}, \end{aligned} \quad (19)$$

where on the right-hand side of Eq. (19) there is just the bound in Eq. (2).

Our calculations lead to

$$\mathcal{B}_{\text{sym}}(\langle J_z \rangle_{\varrho_N}, \langle J_x^2 \rangle_{\varrho_N}) = 6.605 \quad (20)$$

for almost completely polarized spin-squeezed states with  $\alpha = 0.85$ , as well as for not fully polarized ones with  $\alpha = 0.5$ . That is, based on numerics, the left-hand side and the right-hand side of Eq. (19) seem to be equal. This implies that the lower bound, (2), for the quantum Fisher information is optimal for the system. In Appendix G 1, the details of the calculations are given, and we also show examples where we can improve the bound, (2), with our approach, if symmetry is assumed.

## 2. Experiment creating Dicke states

We now present our calculations for an experiment aimed at creating Dicke states in cold gases [39]. The basic ideas are similar to the ones explained in Sec. III D for small systems. The experimental data are  $N = 7900$ ,  $\langle J_z^2 \rangle_N = 112 \pm 31$ ,  $\langle J_x^2 \rangle_N = \langle J_y^2 \rangle_N = 6 \times 10^6 \pm 0.6 \times 10^6$  [21]. Applying some simple transformations, we can obtain a lower bound on  $\mathcal{F}_Q[\varrho_N, J_y]$  for this very large number of particles, even for general, nonsymmetric systems.

For many particles we can make calculations directly only in the symmetric subspace. Thus, we transform the collective quantities such that they are compatible with symmetric states, i.e., they have to fulfill

$$\langle J_x^2 \rangle_{\text{sym}, N} + \langle J_y^2 \rangle_{\text{sym}, N} + \langle J_z^2 \rangle_{\text{sym}, N} = \mathcal{J}_N, \quad (21)$$

where  $\mathcal{J}_N$  is given in Eq. (15). This can be done by multiplying all the second moments by the same number as

$$\langle J_l^2 \rangle_{\text{sym}, N} = \gamma \langle J_l^2 \rangle_N, \quad (22)$$

where  $l = x, y, z$ , and we defined the coefficient

$$\gamma = \frac{\mathcal{J}_N}{\langle J_x^2 + J_y^2 + J_z^2 \rangle_N}. \quad (23)$$

For a symmetric state,  $\gamma = 1$ . In practice,  $\gamma \leq 1$ , but close to 1. From this we can see that there are no symmetric states that are compatible with the experimentally observed expectation values. This is the reason why we needed to apply the transformation (22).

Based on the ideas of Sec. III D, we calculate the lower bound on the quantum Fisher information for symmetric systems, which we denote  $\mathcal{B}_{\text{sym},N}(\langle J_x^2 \rangle_{\text{sym},N}, \langle J_y^2 \rangle_{\text{sym},N}, \langle J_z^2 \rangle_{\text{sym},N})$ .

Finally, to obtain the results for the original, non-symmetric case, we need the following observation.

*Observation 3.* For the bounds for original system and symmetric system, respectively, the inequality

$$\mathcal{B}_N \leq \frac{1}{\gamma} \mathcal{B}_{\text{sym},N} \quad (24)$$

holds, where  $\gamma$  is given in Eq. (23). Here, for brevity we have omitted the arguments of  $\mathcal{B}_N$  and  $\mathcal{B}_{\text{sym},N}$ .

*Proof.* For our proof we need to know that for an  $N$ -qubit singlet state  $\varrho_{\text{singlet},N}$  the relations  $\langle J_l^2 \rangle_{\varrho_{\text{singlet},N}} = 0$  hold for  $l = x, z, y$ . Due to the well-known inequality for the quantum Fisher information  $\mathcal{F}_Q[\varrho_{\text{singlet},N}, J_l] \leq 4(\Delta J_l)^2$ , we have  $\mathcal{F}_Q[\varrho_{\text{singlet},N}, J_y] = 0$ . In other words, the singlet is not useful for metrology with linear interferometers. Let us now consider the mixture

$$\tilde{\varrho}_N = \left(1 - \frac{1}{\gamma}\right) \varrho_{\text{singlet},N} + \frac{1}{\gamma} \varrho_{\text{sym},N}, \quad (25)$$

where  $\varrho_{\text{sym},N}$  is a symmetric state having the second moments  $\langle J_l^2 \rangle_{\text{sym},N}$ . We can easily see from Eq. (22) that for the state  $\tilde{\varrho}_N$ , we have  $\langle J_l^2 \rangle_{\tilde{\varrho}_N} = \langle J_l^2 \rangle_N$ . In other words,  $\tilde{\varrho}_N$  has the same values for the second moments that have been measured experimentally.

We can relate the bound for general systems to the quantum Fisher information for symmetric systems as

$$\mathcal{B}_N \leq \mathcal{F}_Q[\tilde{\varrho}_N, J_y] = \frac{1}{\gamma} \mathcal{F}_Q[\varrho_{\text{sym},N}, J_y]. \quad (26)$$

The inequality in Eq. (26) holds because our bound cannot be larger than the quantum Fisher information of state  $\tilde{\varrho}_N$  having the expectation values  $\langle J_l^2 \rangle_N$ . The equality in Eq. (26) is due to the fact that both  $\tilde{\varrho}_N$  and  $J_y$  can be written as a block-diagonal matrix of blocks corresponding to different eigenvalues of  $J_x^2 + J_y^2 + J_z^2$ . Moreover,  $\varrho_{\text{singlet},N}$  and  $\varrho_{\text{sym},N}$  have nonzero elements in different blocks. Then we can use the general formula [70]

$$\mathcal{F}_Q\left[\bigoplus_k p_k \varrho_k, \bigoplus_k A_k\right] = \sum_k p_k \mathcal{F}_Q[\varrho_k, A_k], \quad (27)$$

where  $\varrho_k$  are density matrices with a unit trace and  $\sum_k p_k = 1$ . ■

Extensive numerics for small systems show Eq. (24) is very close to an equality, hence it can be used as a basis for making calculations for nonsymmetric states. In this way, we arrive at the bound for the experimental system,

$$\frac{\mathcal{B}_N}{N} \approx 2.94. \quad (28)$$

The " $\approx$ " sign is used referring to the fact that we assume that the inequality in Eq. (26) is close to being saturated. The details of the calculations are given in Appendix G 2.

It is instructive to compare the value, (28), to the one obtained in Ref. [21], where the metrological usefulness has been estimated based on the second and fourth moments of the collective angular momentum components, and assuming that  $\langle J_z^2 \rangle$  is used for parameter estimation. The result implies that  $\mathcal{F}_Q[\varrho_N, J_y]/N \geq 3.3$ . Our result in Eq. (28) is somewhat smaller, as we did not use the knowledge of the fourth moment, only the second moments. The closeness of the two results is a strong argument for the correctness of our calculations.

## V. SCALING OF $\mathcal{F}_Q[\varrho, J_l]$ WITH $N$ .

Recent important works examine the scaling of the quantum Fisher information with the particle number for metrology under the presence of decoherence [71]. They consider the quantum Fisher information defined for nonunitary, noisy evolution. They find that for small  $N$  it is close to the value obtained considering coherent dynamics. Hence, even the Heisenberg scaling,  $O(N^2)$ , can be reached. However, if  $N$  is sufficiently large, then, due to the decoherence during the parameter estimation, the quantum Fisher information scales as  $O(N)$ .

In contrast, we do not consider the usefulness of a quantum state in some noisy metrological process, but we estimate the quantum Fisher information assuming a perfect unitary dynamics. Hence, the quantum Fisher information can be smaller than what we expect ideally only due to imperfect state preparation [72]. We can even find simple conditions for the state preparation that lead to a Heisenberg scaling. Based on Eq. (12), if one could realize quantum states  $\varrho_N$  such that  $F_{\text{GHZ}}(\varrho_N) \geq 0.5 + \epsilon$  for  $N \rightarrow \infty$  for some  $\epsilon > 0$ , then we would reach  $\mathcal{F}_Q[\varrho_N, J_z] = O(N^2)$ . Strong numerical evidence suggests that a similar relation holds for the fidelity  $F_{\text{Dicke}}$  and  $\mathcal{F}_Q[\varrho_N, J_y]$ , but with a smaller threshold value for  $F_{\text{Dicke}}$  (see Appendix C). From another point of view, our method can estimate  $\mathcal{F}_Q[\varrho, J_z]$  for large particle numbers, while a direct measurement of the metrological sensitivity considerably underestimates it.

## VI. CONCLUSIONS

We have reported a general method to estimate the metrological usefulness of quantum states based on a few measurements, such as measurements of the fidelity or some collective observables. We tested our approach on extensive experimental data from photonic and cold-gas experiments and demonstrated that it works even for the case of thousands particles [73]. In the future, it would be interesting to use our method to test the optimality of various recent formulas giving a lower bound on the quantum Fisher information [19,22]. Another important question is how to improve the lower bounds on the quantum Fisher information in various experiments by using the knowledge of further operator expectation values.

## ACKNOWLEDGMENTS

We thank S. Altenburg, F. Fröwis, R. Demkowicz-Dobrzański, P. Hyllus, J. Kołodiński, O. Marty, M.W. Mitchell, M. Modugno, L. Pezze, L. Santos, A. Smerzi, I. Urizar-Lanz, and G. Vitagliano for stimulating discussions. We thank the organizers, M. Oberthaler and P. Treutlein, and the participants of the 589. Heraeus-Seminar on “Continuous Variable Entanglement in Atomic Systems” for scientific exchange. We acknowledge the support of the EU (ERC Starting Grant 258647/GEDENTQOPT, ERC Consolidator Grant 683107/TempoQ, CHIST-ERA QUASAR, Marie Curie CIG 293993/ENFOQI, COST Action CA15220), the Spanish Ministry of Economy, Industry and Competitiveness and the European Regional Development Fund FEDER through Grant No. FIS2015-67161-P (MINECO/FEDER), the Basque Government (Project No. IT986-16), the OTKA (Contract No. K83858), the UPV/EHU program UFI 11/55, the FQXi Fund (Grant No. FQXi-RFP-1608), and the DFG (Forschungsstipendium KL 2726/2-1, Project “Precise and efficient characterization of multi-qubit quantum states and gates with trapped ions”).

### Appendix A: Proof of Observation 2

In this section, using Eqs. (4) and (6), we obtain analytically a tight lower bound on the quantum Fisher information based on the fidelity with respect to the GHZ state,  $F_{\text{GHZ}}$ .

The calculation that we have to carry out is computing the bound,

$$\mathcal{B}(F_{\text{GHZ}}) = \sup_r \{r F_{\text{GHZ}} - \sup_\mu [\lambda_{\max}(M_{\text{GHZ}})]\}, \quad (\text{A1})$$

where

$$M_{\text{GHZ}} = r|\text{GHZ}\rangle\langle\text{GHZ}| - 4(J_z - \mu)^2 \mathbf{1}. \quad (\text{A2})$$

We make our calculations in the  $J_z$  basis, which is defined with the  $2^N$  basis vectors  $b_0 = |00\dots 000\rangle$ ,  $b_1 = |00\dots 001\rangle$ ,  $b_2 = |00\dots 010\rangle$ ,  $\dots$ ,  $b_{(2^N-2)} = |11\dots 110\rangle$ , and  $b_{(2^N-1)} = |11\dots 111\rangle$ . It is easy to see that the matrix, (A2), is almost diagonal in the  $J_z$  basis. To be more specific, it can then be written as

$$M_{\text{GHZ}} = M_{2\times 2} \oplus D, \quad (\text{A3})$$

where  $\oplus$  denotes the direct sum and

$$M_{2\times 2} = \begin{pmatrix} \frac{r}{2} - 4(\frac{N}{2} - \mu)^2 & \frac{r}{2} \\ \frac{r}{2} & \frac{r}{2} - 4(\frac{N}{2} + \mu)^2 \end{pmatrix} \quad (\text{A4})$$

is given in the  $\{b_0, b_{(2^N-1)}\}$  basis, while  $D$  is a diagonal matrix given in the basis of the rest of the  $b_k$  vectors as

$$D_k = -4(\langle b_k | J_z | b_k \rangle - \mu)^2 \quad (\text{A5})$$

for  $k = 1, 2, \dots, (2^N - 2)$ . This means that  $M_{\text{GHZ}}$  can be diagonalized as

$$\text{diag}[\lambda_+, \lambda_-, D_1, D_2, \dots, D_{(2^N-2)}], \quad (\text{A6})$$

where the two eigenvalues of  $M_{2\times 2}$  are

$$\lambda_\pm = \frac{r}{2} - N^2 - 4\mu^2 \pm \sqrt{16\mu^2 N^2 + \frac{r^2}{4}}. \quad (\text{A7})$$

Next, we show a way that can simplify our calculations considerably. As indicated in Eq. (A1), we have to look for the maximal eigenvalue of  $M_{\text{GHZ}}$  and then optimize it over  $\mu$ . We exchange the order of the two steps, that is, we look for the maximum of each eigenvalue over  $\mu$  and then find the maximal one. Clearly, based on Eq. (A5) we obtain

$$\sup_\mu D_k = 0, \quad (\text{A8})$$

since we can always choose a value for  $\mu$  that makes  $D_k = 0$ , while it is clear that it cannot be positive. Thus, the maximal eigenvalue, maximized also over  $\mu$ , can be obtained as

$$\begin{aligned} \sup_\mu [\lambda_{\max}(M_{\text{GHZ}})] &:= \max[0, \sup_\mu (\lambda_+)] \\ &= \begin{cases} 0, & \text{if } r < 0, \\ \frac{r}{2} + \frac{r^2}{16N^2}, & \text{if } 0 \leq r \leq 4N^2, \\ -N^2 + r, & \text{if } r > 4N^2, \end{cases} \end{aligned} \quad (\text{A9})$$

where we did not have to look for the maximum of  $\lambda_-$  over  $\mu$  since clearly  $\lambda_+ \geq \lambda_-$ . Finally, we have to substitute Eq. (A9) into Eq. (A1), and carry out the optimization over  $r$ , considering  $F_{\text{GHZ}} \in [0, 1]$ . This way we arrive at Eq. (12). ■

### Appendix B: Calculations in the symmetric subspace

In this section, we prove an important fact, which can be used to simplify our calculations.

*Observation 4.* If a permutationally invariant  $N$ -qubit Hamiltonian  $H$  has a nondegenerate ground state, then the ground state is in the symmetric subspace if  $N > 2$ . An analogous statement holds for the maximal eigenvalue.

*Proof.* This is a well-known fact; we give a proof only for completeness. Let  $|\Psi\rangle$  denote the nondegenerate ground state. This is at the same time the  $T = 0$  thermal ground state, hence it must be a permutationally invariant pure state. For such states  $S_{kl}|\Psi\rangle\langle\Psi|S_{kl} = |\Psi\rangle\langle\Psi|$ , where  $S_{kl}$  is the swap operator exchanging qubits  $k$  and  $l$ . Based on this, it follows that  $S_{kl}|\Psi\rangle = c_{kl}|\Psi\rangle$ , and  $c_{kl} \in \{-1, +1\}$ . There are three possible cases to consider.

(i) All  $c_{kl} = +1$ . In this case, for all permutation operators  $\Pi_j$  we have

$$\Pi_j|\Psi\rangle = |\Psi\rangle, \quad (\text{B1})$$

since any permutation operator  $\Pi_j$  can be constructed as  $\Pi_j = S_{k_1 l_1} S_{k_2 l_2} S_{k_3 l_3} \dots S_{k_m l_m}$ , where  $m \geq 1$ . Equation (B1) means that the state  $|\Psi\rangle$  is symmetric.

(ii) All  $c_{kl} = -1$ . This means that the state is antisymmetric, however, such a state exists only for  $N = 2$  qubits.

(iii) Not all  $c_{kl}$  are identical to each other. In this case, there must be  $k_+, l_+, k_-, l_-$  such that

$$\begin{aligned} S_{k_+l_+}|\Psi\rangle &= +|\Psi\rangle, \\ S_{k_-l_-}|\Psi\rangle &= -|\Psi\rangle. \end{aligned} \quad (\text{B2})$$

Let us assume that  $k_+, l_+, k_-$  and  $l_-$  are indices different from each other. In this case,  $|\Psi'\rangle = S_{k_+k_-}S_{l_+l_-}|\Psi\rangle$  is another ground state of Hamiltonian  $H$  such that

$$\begin{aligned} S_{k_+l_+}|\Psi'\rangle &= -|\Psi'\rangle, \\ S_{k_-l_-}|\Psi'\rangle &= +|\Psi'\rangle. \end{aligned} \quad (\text{B3})$$

Comparing Eq. (B2) and Eq. (B3) we can conclude that  $|\Psi'\rangle \neq |\Psi\rangle$ , while due to the permutational invariance of  $H$  we must have  $\langle\Psi|H|\Psi\rangle = \langle\Psi'|H|\Psi'\rangle$ . Thus,  $|\Psi\rangle$  is not a nongenerate ground state. Let us now see what happens if  $k_+, l_+, k_-$ , and  $l_-$  are not all different from each other. The proof works in an analogous way for the only nontrivial case,  $k_+ = k_-$ , when  $S_{k_+k_-} = \mathbb{1}$ .

Hence, if  $N > 2$ , then only (i) is possible and  $|\Psi\rangle$  must be symmetric. ■

### Appendix C: Estimating the quantum Fisher information based on the fidelity with respect to Dicke states

In this section, we show that if the fidelity with respect to the Dicke state, (C3), is larger than a bound, then  $\mathcal{F}_Q[\varrho, J_y] > 0$ . Moreover, Fig. 1(b) shows that the lower bound on  $\mathcal{F}_Q[\varrho, J_y]$  as a function of the fidelity  $F_{\text{Dicke}}$  normalized by  $N^2$  is not the same curve for all  $N$ . In this section, we demonstrate with numerical evidence that the lower bound normalized by  $N^2$  collapses to a nontrivial curve for large  $N$ .

As the first step, let us consider the state completely polarized in the  $y$  direction,

$$|\Psi_y\rangle = |1\rangle_y^{\otimes N}. \quad (\text{C1})$$

State (C1) does not change under a rotation around the  $y$  axis, hence  $\mathcal{F}_Q[\varrho, J_y] = 0$ . Its fidelity with respect to the Dicke state, (14), is

$$F_{\text{Dicke}}(|\Psi_y\rangle) = \frac{1}{2^N} \binom{N}{N/2} \approx \sqrt{\frac{2}{\pi N}}. \quad (\text{C2})$$

From the convexity of the bound on the quantum Fisher information in  $F_{\text{Dicke}}$ , it immediately follows that for  $F_{\text{Dicke}}$  smaller than Eq. (C2) the optimal lower bound on  $\mathcal{F}_Q[\varrho, J_y]$  will give 0. For the examples shown in Fig. 1(b), this fidelity limit is 0.3125 and 0.1254 for  $N = 6$  and  $N = 40$ , respectively.

Next, we examine what happens if the fidelity is larger than Eq. (C2).

*Observation 5.* If for some state  $\varrho$  we have

$$F_{\text{Dicke}}(\varrho) \equiv \text{Tr}(|D_N\rangle\langle D_N|\varrho) > F_{\text{Dicke}}(|\Psi_y\rangle), \quad (\text{C3})$$

then  $\mathcal{F}_Q[\varrho, J_y] > 0$ . [The state  $|D_N\rangle$  is given in Eq. (14), and  $F_{\text{Dicke}}(|\Psi_y\rangle)$  is given in Eq. (C2).]

*Proof.* We have to determine the maximum for  $F_{\text{Dicke}}(\varrho)$  for states that are not useful for metrology, i.e.,  $\mathcal{F}_Q[\varrho, J_y] = 0$ . We

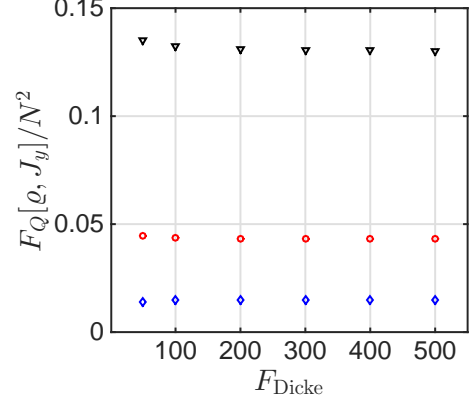


FIG. 4. (Color online) The lower bound on  $\mathcal{F}_Q[\varrho, J_y]$ , denoted  $\mathcal{B}(F_{\text{Dicke}})$ , for various particle numbers, for  $F_{\text{Dicke}} = 0.2$  (diamonds), 0.5 (circles), and 0.7 (triangles). For  $F_{\text{Dicke}} = 0.2$ , 10 the calculated values times 10 are shown, for better visibility.

know that  $\mathcal{F}_Q[\varrho, J_y]$  is the convex roof of  $4(\Delta J_y)^2$  [51]. Hence, if we have a mixed state for which  $\mathcal{F}_Q[\varrho, J_y] = 0$ , then it can always be decomposed into the mixture of pure states  $|\Psi_k\rangle$  for which  $\mathcal{F}_Q[\Psi_k, J_y] = 0$ . As a consequence, the extremal states of the set of states for which  $\mathcal{F}_Q[\varrho, J_y] = 0$  are pure states, and we can restrict our search for pure states. The optimization problem we have to solve can be given as

$$\max_{|\Psi\rangle: \mathcal{F}_Q[|\Psi\rangle, J_y]=0} |\langle\Psi|D_N\rangle|^2. \quad (\text{C4})$$

Pure states  $|\Psi\rangle$  for which  $\mathcal{F}_Q[|\Psi\rangle, J_y] = 0$  must be invariant under  $U_\phi = \exp(-iJ_y\phi)$  for any  $\phi$ . Such states are the eigenstates of  $J_y$ . In order to maximize the overlap with the symmetric Dicke state  $|D_N\rangle$  in Eq. (C4), we have to look for symmetric eigenstates of  $J_y$ . These are the symmetric Dicke states in the  $y$  basis  $|D_N^{(m)}\rangle_y$ . [See Eq. (13).] In order to proceed, we have to write down  $|D_N^{(m)}\rangle_y$  in the  $z$  basis. Then, using the formula

$$\sum_k \binom{n}{k} \binom{n}{q-k} (-1)^k = \begin{cases} \binom{n}{q/2} (-1)^{q/2} & \text{for even } N, \\ 0 & \text{for odd } N, \end{cases} \quad (\text{C5})$$

one finds that the squared overlap is given by

$$|\langle D_N^{(N/2)} | D_N^{(m)} \rangle_y|^2 = \begin{cases} \frac{\binom{N/2}{m/2} \binom{N/2}{N/2}}{2^N \binom{N}{m}} & \text{for even } N, \\ 0 & \text{for odd } N, \end{cases} \quad (\text{C6})$$

which is maximal for  $m = 0$ . ■

Next, we examine the behavior of our lower bound on  $\mathcal{F}_Q[\varrho, J_y]$  based on  $F_{\text{Dicke}}$  for large  $N$ . In Fig. 4, the calculations up to  $N = 500$  present strong evidence that for the fidelity values  $F_{\text{Dicke}} = 0.2, 0.5$ , and 0.8 the lower bound on the quantum Fisher information  $\mathcal{F}_Q[\varrho, J_y]$  has an  $O(N^2)$  scaling. If this is correct, then reaching a fidelity larger than a certain bound for large  $N$  would imply Heisenberg scaling for the bound on the quantum Fisher information. Note that it is difficult to present similar numerical evidence for small values of  $F_{\text{Dicke}}$ , since in that case the bound for the quantum Fisher information is nonzero only for large  $N$  due to Observation 5.

#### Appendix D: Boundary of physical states in the $(\langle J_z \rangle, \langle J_x^2 \rangle)$ -plane.

In this section, we discuss how to find the physical region in the  $(\langle J_z \rangle, \langle J_x^2 \rangle)$  plane, which was used to prepare Fig. 2(a).

The physical region must be a convex one, since the set of quantum states is convex and the coordinates depend linearly on the density matrix. Hence, we look for the minimal or maximal  $\langle J_x^2 \rangle$  for a given  $\langle J_z \rangle$  by looking for the ground states of the Hamiltonians [59],

$$H_{\text{bnd}}^{(\pm)}(\mu) = \pm J_x^2 - \mu J_z. \quad (\text{D1})$$

The points of the boundary can be obtained by evaluating  $\langle J_x^2 \rangle$  and  $\langle J_z \rangle$  for the ground states of Eq. (D1). In particular, the ground states of  $H_{\text{bnd}}^{(+)}$  correspond to boundary points below point P corresponding to the fully polarized state in Fig. 2(a). The ground states of  $H_{\text{bnd}}^{(-)}$  correspond to boundary points above point P.

For  $0 < \mu < \infty$ , the Hamiltonian  $H_{\text{bnd}}^{(+)}$  has nondegenerate ground states with  $\langle J_x \rangle = 0$ . For even  $N$ , the ground state of  $H_{\text{bnd}}^{(+)}$  minimizes both  $\langle J_x^2 \rangle$  and  $(\Delta J_x)^2$  for a given  $\langle J_z \rangle$ . For odd  $N$ , this is not the case for small  $\mu$  [59].

On the other hand,  $H_{\text{bnd}}^{(-)}$  has doubly degenerate ground states. For the ground-state subspace, we have  $\langle J_x \rangle = 0$ . Hence, for both even  $N$  and odd  $N$ , the ground state of  $H_{\text{bnd}}^{(-)}$  maximizes both  $\langle J_x^2 \rangle$  and  $(\Delta J_x)^2$  for a given  $\langle J_z \rangle$ .

#### Appendix E: Quantum Fisher information for states at the boundary of the physical region in the $(\langle J_z \rangle, \langle J_x^2 \rangle)$ -plane

We show that, for even  $N$ , the ground states of  $H_{\text{bnd}}^{(+)}$  defined in Eq. (D1) are close to saturating Eq. (2). As a consequence, for the boundary of the physical region in the  $(\langle J_z \rangle, \langle J_x^2 \rangle)$  plane below point P in Fig. 2, bound (2) is close to the optimal lower bound.

We carry out numerical calculations. Let us denote by  $|\Psi_\mu\rangle$  the ground state of  $H_{\text{bnd}}^{(+)}$ . Moreover, let us denote the relevant expectation values for this state  $\langle J_x^2 \rangle_\mu$  and  $\langle J_z \rangle_\mu$ . We know that under the constraint  $\langle J_z \rangle = \langle J_z \rangle_\mu$ , the state  $|\Psi_\mu\rangle$  minimizes  $\langle J_x^2 \rangle$ . For  $H_{\text{bnd}}^{(-)}$ , the ground state is unique for  $0 < \mu < \infty$ . Thus, there is no other quantum state with the same value for  $\langle J_z \rangle$  and  $\langle J_x^2 \rangle$ .

There is a very important consequence of the uniqueness of the ground state of  $H_{\text{bnd}}^{(+)}$  for the lower bound on the quantum Fisher information. We have discussed that our method based on the Legendre transform gives the optimal lower bound for the quantum Fisher information

$$\mathcal{F}_Q[\varrho, J_y] \geq \mathcal{B}(\langle J_z \rangle_\varrho, \langle J_x^2 \rangle_\varrho), \quad (\text{E1})$$

where  $\mathcal{B}$  denotes the optimal bound. Since there is a unique state corresponding to the boundary points, we must have for the states at the boundary

$$\mathcal{B}(\langle J_z \rangle_\mu, \langle J_x^2 \rangle_\mu) = \mathcal{F}_Q[|\Psi_\mu\rangle, J_y]. \quad (\text{E2})$$

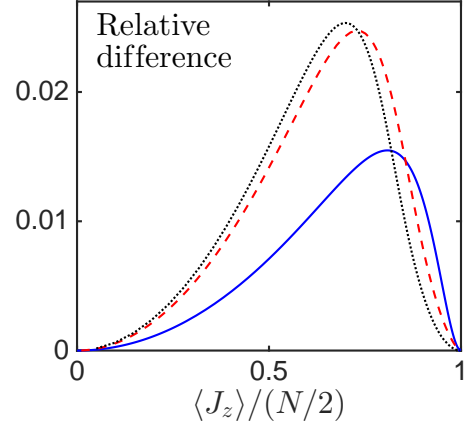


FIG. 5. Behavior of the bound in Eq. (2) for points at the boundary of physical states. The relative difference with respect to the optimal lower bound is plotted for  $N = 4$  (solid line),  $N = 20$  (dashed line), and  $N = 1000$  (dotted line).

Thus, for the boundary points we do not have to compute the lower bound with the method based on the Legendre transform. We can just calculate the right-hand side of Eq. (E2) instead. Since we have a pure state, the quantum Fisher information is proportional to the variance  $\mathcal{F}_Q[\varrho, J_y] = 4(\Delta J_y)^2$  [11].

We add that, for even  $N$ , state  $|\Psi_\mu\rangle$  not only minimizes  $\langle J_x^2 \rangle$  for a given value of  $\langle J_z \rangle$ , but also minimizes  $(\Delta J_x)^2$ , and this state is unique [59]. Hence, for the points on the boundary of physical states in the  $(\langle J_z \rangle, (\Delta J_x)^2)$ -space we have

$$\mathcal{B}(\langle J_z \rangle_\mu, (\Delta J_x)_\mu^2) = \mathcal{F}_Q[|\Psi_\mu\rangle, J_y], \quad (\text{E3})$$

where  $\mathcal{B}$  denotes the optimal bound if the expectation value  $\langle J_z \rangle$  and the variance  $(\Delta J_x)^2$  are constrained. Note that bound (E3) is monotonous in  $(\Delta J_x)_\mu^2$  [59].

In Fig. 5, we plot the relative difference between the quantum Fisher information of  $|\Psi_\mu\rangle$  and the lower bound (2) given as

$$\frac{\mathcal{F}_Q[|\Psi_\mu\rangle, J_y] - \frac{\langle J_z \rangle_\mu^2}{(\Delta J_x)_\mu^2}}{\mathcal{F}_Q[|\Psi_\mu\rangle, J_y]} \quad (\text{E4})$$

for various particle numbers. It can be seen that for an almost fully polarized state the difference is small, but even for a state that is not fully polarized the relative difference is smaller than 3% for the particle numbers considered.

#### Appendix F: Why we can assume $\langle J_x \rangle = 0$ for the discussion of spin-squeezed states

We show that for the state minimizing  $\mathcal{F}_Q[\varrho, J_y]$  for given  $\langle J_z \rangle$  and  $\langle J_x^2 \rangle$  we have  $\langle J_x \rangle = 0$ . Hence, if we constrain only  $\langle J_z \rangle$  and  $\langle J_x^2 \rangle$ , then we get the same bound as if we constrained  $\langle J_z \rangle$  and  $\langle J_x^2 \rangle$ , and we used an additional constraint  $\langle J_x \rangle = 0$ .

For spin-squeezed states, we have to solve the following optimization task. We have to find a tight lower bound on the quantum Fisher information

$$\mathcal{F}_Q[\varrho, J_y] \geq \mathcal{B}(\vec{w}_\varrho) \quad (\text{F1})$$

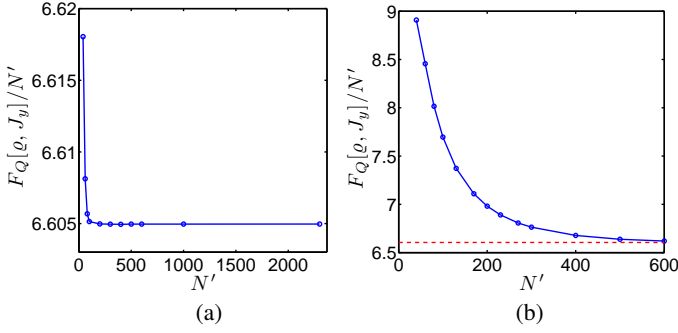


FIG. 6. (Color online) Lower bound on the quantum Fisher information based on  $\langle J_z \rangle$  and  $(\Delta J_x)^2$  obtained for different particle numbers making calculations in the symmetric subspace.  $N = 2300$  corresponds to the spin-squeezing experiment in Ref. [7]. (a) Almost fully polarized spin-squeezed state. Even for a moderate  $N'$ , the bound is practically identical to the right-hand side of Eq. (18). (b) Spin-squeezed state that is not fully polarized. For large  $N'$ , the bound converges to the right-hand side of Eq. (18), represented by the dashed line. In both panels, circles correspond to the results of our calculations, which are connected by straight lines to guide the eye.

where  $\vec{w}_\varrho = (\langle J_z \rangle_\varrho, \langle J_x^2 \rangle_\varrho, \langle J_x \rangle_\varrho)$ . For any  $\varrho$ , we can define a state  $\varrho_- = \sigma_z^{\otimes N} \varrho \sigma_z^{\otimes N}$ , for which  $\vec{w}_{\varrho_-} = (\langle J_z \rangle_\varrho, \langle J_x^2 \rangle_\varrho, -\langle J_x \rangle_\varrho)$ . The metrological usefulness of  $\varrho$  and  $\varrho_-$  are the same, i.e.,  $\mathcal{F}_Q[\varrho, J_y] = \mathcal{F}_Q[\varrho_-, J_y]$ . Then, for any  $\varrho$ , we can define a state  $\varrho_0 = \frac{1}{2}(\varrho + \varrho_-)$ , for which we have  $\vec{w}_{\varrho_0} = (\langle J_z \rangle_\varrho, \langle J_x^2 \rangle_\varrho, 0)$ . Due to the convexity of the quantum Fisher information,  $\varrho_0$  cannot be better metrologically than  $\varrho$  or  $\varrho_-$ , that is,  $\mathcal{F}_Q[\varrho, J_y] = \mathcal{F}_Q[\varrho_-, J_y] \geq \mathcal{F}_Q[\varrho_0, J_y]$ .

Since for any  $\varrho$  there is a corresponding  $\varrho_0$  with the above properties, it follows that  $\mathcal{B}(\vec{v}_\varrho) = \mathcal{B}(\vec{v}_{\varrho_-}) \geq \mathcal{B}(\vec{w}_{\varrho_0}) = \mathcal{B}(\langle J_z \rangle_\varrho, \langle J_x^2 \rangle_\varrho, 0)$ . Thus, the worst-case bound for given  $\langle J_z \rangle$  and  $\langle J_x^2 \rangle$  is  $\mathcal{B}(\langle J_z \rangle, \langle J_x^2 \rangle, 0)$ . Hence,

$$\mathcal{B}(\langle J_z \rangle, \langle J_x^2 \rangle) = \mathcal{B}(\langle J_z \rangle, \langle J_x^2 \rangle, \langle J_x \rangle = 0), \quad (\text{F2})$$

and our claim is proved.

## Appendix G: Many-particle experiments

In this section, we consider cold-gas experiments creating spin-squeezed states and Dicke states.

### 1. Spin-squeezing experiment

We now give the details of the calculations described in Sec. IV B 1. We present a simple scheme that we need to handle large systems. We do not make calculations directly for  $N = 2300$ , but we start with smaller systems and make calculations for larger and larger system sizes. This is motivated as follows. First, we can use the output of an optimization for a smaller particle number as an initial guess for a larger particle number. Thus, we need fewer steps for the numerical optimization for large system sizes, which makes our computations faster. Second, while we are able to carry out the calculation

for the particle number of the experiment, we also see that we could even extrapolate the results from the results obtained for lower particle numbers. This is useful for future application of our method to very large systems.

The basic idea is that we transform the collective quantities from  $N$  to a smaller particle number  $N'$  using the scaling relation

$$\begin{aligned} \langle J_z \rangle &= \frac{N'}{2} \alpha, \\ (\Delta J_x)^2 &= \xi_s^2 \frac{N'}{4} \alpha^2. \end{aligned} \quad (\text{G1})$$

We see that for the scaling we consider, for all  $N'$  the bound in Eq. (2) is obtained as

$$\frac{\mathcal{F}_Q[\varrho_{N'}, J_y]}{N'} \geq \frac{1}{\xi_s^2} = 6.605. \quad (\text{G2})$$

where  $\varrho_{N'}$  is a state satisfying Eq. (G1). Let us first take  $\alpha = 0.85$ , which is somewhat lower than the experimental value, however, it helps us to see various characteristics of the method. At the end of the section we also discuss the results for other values of  $\alpha$ . Based on these ideas, we compute the bound  $\mathcal{B}_{\text{sym}}(\langle J_z \rangle_{\varrho_{N'}}, \langle J_x^2 \rangle_{\varrho_{N'}})$ , described in Sec. IV B 1, for the quantum Fisher information for an increasing system size  $N'$ .

The results are shown in Fig. 6(a). The bound obtained in this way is close to the bound in Eq. (18) even for small  $N'$ . For a larger particle number, i.e.,  $N' > 200$ , it is constant and coincides with the bound in Eq. (18). This also strongly supports the idea that we could have used the results from small particle numbers to extrapolate the bound for  $N$ . Since for the experimental particle numbers we obtain that  $\mathcal{B}_{\text{sym}}(\langle J_z \rangle_{\varrho_N}, \langle J_x^2 \rangle_{\varrho_N})$  equals the bound in (2), we find that for  $N' = N$  all three lower bounds in Eq. (19) must be equal. Hence, Eq. (2) is optimal for the experimental system considered in this section. Besides, these results also present a strong argument for the correctness of our approach.

We now give more details of the calculation. We were able to carry out the optimization up to  $N' = 2300$  with a usual laptop computer using the MATLAB programming language [74]. We started the calculation for each given particle number with the  $r_k$  parameters obtained for the previous simulation with a smaller particle number.

Let us consider a spin-squeezed state that is not fully polarized and  $\alpha = 0.5$ . In Fig. 6(b), we can see that for small particle numbers we have a bound on  $\mathcal{F}_Q[\varrho, J_y]$  larger than the one obtained from Eq. (2). Thus for this case we could improve bound (2) by assuming symmetry. On the other hand, for large particle numbers we approach Eq. (2).

After seeing the results of the calculations for  $\alpha = 0.85$  and  $\alpha = 0.5$ , the question arises, what would the result be for larger  $\alpha$ , that is, for even more polarized states? It turns out that if we choose  $\alpha$  larger than 0.85, then the convergence of  $\mathcal{F}_Q[\varrho_{N'}, J_y]/N'$  will be even faster than in Fig. 6(a), and for the particle number of the experiment we obtain again that Eq. (2) is saturated.

Finally, we add a note on a technical detail. We carried out our calculations with the constraints on  $(\Delta J_x)^2$ , and  $\langle J_z \rangle$ , with the additional constraint  $\langle J_x \rangle = 0$ . For the experimental particle numbers, one can show that our results are valid even if we

constrain only  $(\Delta J_x)^2$  and  $\langle J_z \rangle$ , and do not use the  $\langle J_x \rangle = 0$  constraint. This way, in principle, we can only get a bound that is equal to or lower than one we obtained before. However, we previously obtained a value identical to the analytical bound, (2). The optimal bound cannot be below the analytic bound, since then the analytic bound would overestimate the quantum Fisher information, and it would not be a valid bound. Hence, even an optimization without the  $\langle J_x \rangle = 0$  constraint could not obtain a smaller value than our results.

## 2. Experiment creating Dicke states

We now give the details for the calculations described in Sec. IV B 2. As in Appendix G 1, we compute the bound for quantum Fisher information for an increasing system size  $N'$ . However, now we are not able to do the calculation for the experimental particle number, and we use extrapolation from the results obtained for smaller particle numbers.

First, we transform the measured second moments to values corresponding to a symmetric system using Eq. (22) and Eq. (23). For our case,  $\gamma = 1.301$ . In this way, we obtain

$$\begin{aligned} \langle J_z^2 \rangle_{\text{sym}, N} &= 145.69, \\ \langle J_x^2 \rangle_{\text{sym}, N} &= \langle J_y^2 \rangle_{\text{sym}, N} = 7.8 \times 10^6. \end{aligned} \quad (\text{G3})$$

Next, we carry out calculations for symmetric systems. We consider a scaling that keeps expectation values such that the corresponding quantum state must be symmetric. Hence, we use the relations

$$\begin{aligned} \langle J_z^2 \rangle_{\text{sym}, N'} &= \langle J_z^2 \rangle_{\text{sym}, N}, \\ \langle J_x^2 \rangle_{\text{sym}, N'} &= \langle J_y^2 \rangle_{\text{sym}, N'} = \frac{1}{2}(\mathcal{J}_{N'} - \langle J_z^2 \rangle_{\text{sym}, N'}), \end{aligned} \quad (\text{G4})$$

where  $\mathcal{J}_{N'}$  is defined in Eq. (15). Note that with Eq. (G4),  $\langle J_x^2 + J_y^2 + J_z^2 \rangle_{\text{sym}, N'} = \mathcal{J}_{N'}$  holds for all  $N'$ , hence the state must be symmetric. The main characteristics of the scaling relation, Eq. (G4), can be summarized as follows.  $\langle J_z^2 \rangle_{\text{sym}, N'}$  remains equal to  $\langle J_z^2 \rangle_{\text{sym}, N}$ , while  $\langle J_x^2 \rangle_{\text{sym}, N'}$  and  $\langle J_y^2 \rangle_{\text{sym}, N'}$  are chosen such that they are equal to each other and the state is symmetric. For large  $N$ , Eq. (G4) implies a scaling of  $\langle J_z^2 \rangle \sim \text{const.}$  and  $\langle J_x^2 \rangle = \langle J_y^2 \rangle \sim N(N+2)/8$ .

Let us now turn to the central quantities of our paper, the lower bounds on the quantum Fisher information. The quantum Fisher information for the experimentally obtained state  $\varrho_N$  is bounded from below as

$$\mathcal{F}_Q[\varrho_N, J_y] \geq \mathcal{B}_N, \quad (\text{G5})$$

where  $\mathcal{B}_N$  denotes a bound based on  $\langle J_l^2 \rangle_N$  for  $l = x, y, z$ . An analogous relation for the symmetric state  $\varrho_{\text{sym}, N'}$  is

$$\mathcal{F}_Q[\varrho_{\text{sym}, N'}, J_y] \geq \mathcal{B}_{\text{sym}, N'}, \quad (\text{G6})$$

where  $\mathcal{B}_{\text{sym}, N'}$  denotes a bound based on  $\langle J_l^2 \rangle_{\text{sym}, N'}$  for  $l = x, y, z$ .

A central point in our scheme is that due to the scaling properties of the system we can obtain the value for the particle

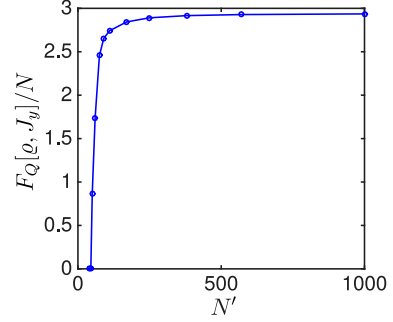


FIG. 7. (Color online) Quantum Fisher information extrapolated to  $N = 7900$  from calculations with different particle numbers  $N'$  in an experiment creating Dicke states. Circles correspond to the results of our calculations, which are connected by straight lines to guide the eye.

number  $N$  from the value for a smaller particle number  $N'$  as [19]

$$\mathcal{B}_{\text{sym}, N} \approx \frac{\mathcal{J}_N}{\mathcal{J}_{N'}} \mathcal{B}_{\text{sym}, N'}, \quad (\text{G7})$$

which we verify numerically. Note that for large  $N$ , we have  $\mathcal{J}_N/\mathcal{J}_{N'} \sim N^2/(N')^2$ .

As the last step, we have to return from the symmetric system to our real, not fully symmetric one. Based on Eq. (G7), and assuming that Eq. (24) is close to being saturated, a relation for the lower bound for the original problem can be obtained from the bound on the symmetric problem with  $N'$  particles as

$$\mathcal{B}_N \approx \frac{1}{\gamma} \frac{\mathcal{J}_N}{\mathcal{J}_{N'}} \mathcal{B}_{\text{sym}, N'}. \quad (\text{G8})$$

In Fig. 7, we plot the right-hand side of Eq. (G8) as a function of  $N'$ . We can see that  $\mathcal{B}_{N'}$  is constant or slightly increasing for  $N' > 400$ . This is strong evidence that Eq. (G7) is valid for large particle numbers. With this, we arrive at Eq. (28).

[1] R. Horodecki, P. Horodecki, M. Horodecki, and K. Horodecki, *Rev. Mod. Phys.* **81**, 865 (2009).  
 [2] O. Guhne and G. Toth, *Phys. Rep.* **474**, 1 (2009).

[3] L. Pezze and A. Smerzi, *Phys. Rev. Lett.* **102**, 100401 (2009).  
 [4] A. Louchet-Chauvet, J. Appel, J. J. Renema, D. Oblak, N. Kjaergaard, and E. S. Polzik, *New J. Phys.* **12**, 065032 (2010).

- [5] J. Appel, P. J. Windpassinger, D. Oblak, U. B. Hoff, N. Kjørgaard, and E. S. Polzik, *PNAS* **106**, 10960 (2009).
- [6] M. F. Riedel, P. Böhi, Y. Li, T. W. Hänsch, A. Sinatra, and P. Treutlein, *Nature* **464**, 1170 (2010).
- [7] C. Gross, T. Zibold, E. Nicklas, J. Esteve, and M. K. Oberthaler, *Nature* **464**, 1165 (2010).
- [8] B. Lücke, M. Scherer, J. Kruse, L. Pezzé, F. Deuretzbacher, P. Hyllus, J. Peise, W. Ertmer, J. Arlt, L. Santos, A. Smerzi, and C. Klempt, *Science* **334**, 773 (2011).
- [9] H. Strobel, W. Muessel, D. Linnemann, T. Zibold, D. B. Hume, L. Pezzé, A. Smerzi, and M. K. Oberthaler, *Science* **345**, 424 (2014).
- [10] P. Hyllus, O. Gühne, and A. Smerzi, *Phys. Rev. A* **82**, 012337 (2010).
- [11] V. Giovannetti, S. Lloyd, and L. Maccone, *Science* **306**, 1330 (2004); M. G. A. Paris, *Int. J. Quant. Inf.* **07**, 125 (2009); R. Demkowicz-Dobrzanski, M. Jarzyna, and J. Kolodnyski, *Prog. Optics* **60**, 345 (2015), [arXiv:1405.7703](https://arxiv.org/abs/1405.7703); L. Pezze and A. Smerzi, in *Atom Interferometry (Proc. Int. School of Physics 'Enrico Fermi', Course 188, Varenna)*, edited by G. Tino and M. Kasevich (IOS Press, Amsterdam, 2014) pp. 691–741, [arXiv:1411.5164](https://arxiv.org/abs/1411.5164).
- [12] C. Helstrom, *Quantum Detection and Estimation Theory* (Academic Press, New York, 1976); A. Holevo, *Probabilistic and Statistical Aspects of Quantum Theory* (North-Holland, Amsterdam, 1982); S. L. Braunstein and C. M. Caves, *Phys. Rev. Lett.* **72**, 3439 (1994); D. Petz, *Quantum information theory and quantum statistics* (Springer, Berlin, Heilderberg, 2008); S. L. Braunstein, C. M. Caves, and G. J. Milburn, *Ann. Phys.* **247**, 135 (1996).
- [13] P. Hyllus, W. Laskowski, R. Krschek, C. Schwemmer, W. Wieczorek, H. Weinfurter, L. Pezzé, and A. Smerzi, *Phys. Rev. A* **85**, 022321 (2012); G. Tóth, *Phys. Rev. A* **85**, 022322 (2012).
- [14] R. Krschek, C. Schwemmer, W. Wieczorek, H. Weinfurter, P. Hyllus, L. Pezzé, and A. Smerzi, *Phys. Rev. Lett.* **107**, 080504 (2011).
- [15] In another context, the measurement of the quantum Fisher information has recently been considered in systems in thermal equilibrium. P. Hauke, M. Heyl, L. Tagliacozzo, and P. Zoller, *Nat. Phys.* **12**, 778 (2016); T. Shitara and M. Ueda, *Phys. Rev. A* **94**, 062316 (2016).
- [16] L. Pezze, Y. Li, W. Li, and A. Smerzi, *PNAS* **113**, 11459 (2016).
- [17] F. Fröwis, P. Sekatski, and W. Dür, *Phys. Rev. Lett.* **116**, 090801 (2016).
- [18] R. H. Dicke, *Phys. Rev.* **93**, 99 (1954).
- [19] Z. Zhang and L. M. Duan, *New J. Phys.* **16**, 103037 (2014).
- [20] F. Fröwis, R. Schmied, and N. Gisin, *Phys. Rev. A* **92**, 012102 (2015).
- [21] I. Apellaniz, B. Lücke, J. Peise, C. Klempt, and G. Tóth, *New J. Phys.* **17**, 083027 (2015).
- [22] E. Oudot, P. Sekatski, F. Fröwis, N. Gisin, and N. Sangouard, *J. Opt. Soc. Am. B* **32**, 2190 (2015).
- [23] M. Kitagawa and M. Ueda, *Phys. Rev. A* **47**, 5138 (1993); D. J. Wineland, J. J. Bollinger, W. M. Itano, and D. J. Heinzen, *Phys. Rev. A* **50**, 67 (1994).
- [24] D. M. Greenberger, M. A. Horne, A. Shimony, and A. Zeilinger, *Am. J. Phys.* **58**, 1131 (1990).
- [25] D. Bouwmeester, J.-W. Pan, M. Daniell, H. Weinfurter, and A. Zeilinger, *Phys. Rev. Lett.* **82**, 1345 (1999).
- [26] J.-W. Pan, D. Bouwmeester, M. Daniell, H. Weinfurter, and A. Zeilinger, *Nature* **403**, 515 (2000).
- [27] Z. Zhao, T. Yang, Y.-A. Chen, A.-N. Zhang, M. Żukowski, and J.-W. Pan, *Phys. Rev. Lett.* **91**, 180401 (2003).
- [28] C.-Y. Lu, X.-Q. Zhou, O. Gühne, W.-B. Gao, J. Zhang, Z.-S. Yuan, A. Goebel, T. Yang, and J.-W. Pan, *Nat. Phys.* **3**, 91 (2007).
- [29] W.-B. Gao, C.-Y. Lu, X.-C. Yao, P. Xu, O. Gühne, A. Goebel, Y.-A. Chen, C.-Z. Peng, Z.-B. Chen, and J.-W. Pan, *Nat. Phys.* **6**, 331 (2010).
- [30] D. Leibfried, M. Barrett, T. Schaetz, J. Britton, J. Chiaverini, W. Itano, J. Jost, C. Langer, and D. Wineland, *Science* **304**, 1476 (2004).
- [31] C. Sackett, D. Kielpinski, B. King, C. Langer, V. Meyer, C. Myatt, M. Rowe, Q. Turchette, W. Itano, D. Wineland, and C. Monroe, *Nature* **404**, 256 (2000).
- [32] T. Monz, P. Schindler, J. T. Barreiro, M. Chwalla, D. Nigg, W. A. Coish, M. Harlander, W. Hänsel, M. Hennrich, and R. Blatt, *Phys. Rev. Lett.* **106**, 130506 (2011).
- [33] N. Kiesel, C. Schmid, G. Tóth, E. Solano, and H. Weinfurter, *Phys. Rev. Lett.* **98**, 063604 (2007).
- [34] W. Wieczorek, R. Krschek, N. Kiesel, P. Michelberger, G. Tóth, and H. Weinfurter, *Phys. Rev. Lett.* **103**, 020504 (2009).
- [35] R. Prevedel, G. Cronenberg, M. S. Tame, M. Paternostro, P. Walther, M. S. Kim, and A. Zeilinger, *Phys. Rev. Lett.* **103**, 020503 (2009).
- [36] A. Chiuri, C. Greganti, M. Paternostro, G. Vallone, and P. Mataloni, *Phys. Rev. Lett.* **109**, 173604 (2012).
- [37] P. Schindler, M. Müller, D. Nigg, J. T. Barreiro, E. Martinez, M. Hennrich, T. Monz, S. Diehl, P. Zoller, and R. Blatt, *Nat. Phys.* **9**, 361 (2013).
- [38] C. Gross, *J. Phys. B: At. Mol. Opt. Phys.* **45**, 103001 (2012); J. Ma, X. Wang, C. P. Sun, and F. Nori, *Phys. Rep.* **509**, 89 (2011); J. Hald, J. L. Sørensen, C. Schori, and E. S. Polzik, *Phys. Rev. Lett.* **83**, 1319 (1999); S. R. de Echaniz, M. W. Mitchell, M. Kubasik, M. Koschorreck, H. Crepaz, J. Eschner, and E. S. Polzik, *J. Opt. B: Quantum and Semiclassical Opt.* **7**, S548 (2005); R. J. Sewell, M. Koschorreck, M. Napolitano, B. Dubost, N. Behbood, and M. W. Mitchell, *Phys. Rev. Lett.* **109**, 253605 (2012).
- [39] B. Lücke, J. Peise, G. Vitagliano, J. Arlt, L. Santos, G. Tóth, and C. Klempt, *Phys. Rev. Lett.* **112**, 155304 (2014).
- [40] C. Hamley, C. Gerving, T. Hoang, E. Bookjans, and M. Chapman, *Nat. Phys.* **8**, 305 (2012).
- [41] X.-Y. Luo, Y.-Q. Zou, L.-N. Wu, Q. Liu, M.-F. Han, M. K. Tey, and L. You, *Science* **355**, 620 (2017).
- [42] A. Sørensen, L.-M. Duan, J. Cirac, and P. Zoller, *Nature* **409**, 63 (2001).
- [43] J. K. Korbicz, J. I. Cirac, and M. Lewenstein, *Phys. Rev. Lett.* **95**, 120502 (2005).
- [44] G. Tóth, C. Knapp, O. Gühne, and H. J. Briegel, *Phys. Rev. Lett.* **99**, 250405 (2007).
- [45] A. C. Doherty, P. A. Parrilo, and F. M. Spedalieri, *Phys. Rev. Lett.* **88**, 187904 (2002).
- [46] H. Wunderlich and M. B. Plenio, *J. Mod. Opt.* **56**, 2100 (2009).
- [47] G. Tóth, T. Moroder, and O. Gühne, *Phys. Rev. Lett.* **114**, 160501 (2015).
- [48] R. T. Rockafellar, *Convex analysis* (Princeton University Press, Princeton, 1997).
- [49] O. Gühne, M. Reimpell, and R. F. Werner, *Phys. Rev. Lett.* **98**, 110502 (2007).
- [50] J. Eisert, F. G. S. L. Brandao, and K. M. R. Audenaert, *New J. Phys.* **9**, 46 (2007).
- [51] G. Tóth and D. Petz, *Phys. Rev. A* **87**, 032324 (2013); S. Yu, [arXiv:1302.5311](https://arxiv.org/abs/1302.5311).
- [52] An alternative definition is  $\mathcal{F}_Q(W) = \sup_{\psi_v} \langle W \rangle_{\psi_v} - 4(\Delta J)_{\psi_v}^2$ , where  $|\psi_v\rangle$  is the eigenstate with the maximal eigenvalue of the

- operator  $W - 4J_I^2 - \nu J_I$ . In certain cases, this form can be calculated numerically more easily than Eq. (6).
- [53] A. Luis, *Physics Letters A* **329**, 8 (2004).
- [54] S. Boixo, S. T. Flammia, C. M. Caves, and J. Geremia, *Phys. Rev. Lett.* **98**, 090401 (2007).
- [55] S. Choi and B. Sundaram, *Phys. Rev. A* **77**, 053613 (2008).
- [56] S. M. Roy and S. L. Braunstein, *Phys. Rev. Lett.* **100**, 220501 (2008).
- [57] M. Napolitano, M. Koschorreck, B. Dubost, N. Behbood, R. Sewell, and M. W. Mitchell, *Nature* **471**, 486 (2011).
- [58] M. J. W. Hall and H. M. Wiseman, *Phys. Rev. X* **2**, 041006 (2012).
- [59] A. S. Sørensen and K. Mølmer, *Phys. Rev. Lett.* **86**, 4431 (2001).
- [60] A not tight lower bounds on the quantum Fisher based on the fidelity has been presented in R. Augusiak, J. Kołodyński, A. Streltsov, M. N. Bera, A. Acín, and M. Lewenstein, *Phys. Rev. A* **94**, 012339 (2016).
- [61] G. Tóth, *J. Opt. Soc. Am. B* **24**, 275 (2007).
- [62] G. Tóth, W. Wieczorek, R. Krischek, N. Kiesel, P. Michelberger, and H. Weinfurter, *New J. Phys.* **11**, 083002 (2009).
- [63] M. J. Holland and K. Burnett, *Phys. Rev. Lett.* **71**, 1355 (1993).
- [64] Due to symmetries of the problem, when minimizing  $\mathcal{F}_Q[\rho, J_y]$  with the constrains on  $\langle J_z \rangle$  and  $\langle J_x^2 \rangle$ , we do not have to add explicitly the constraint  $\langle J_x \rangle = 0$ . Optimization with only the first two constraints will give the same bound (see Appendix F).
- [65] Outside the symmetric subspace, there are other states with  $\langle J_z \rangle = \langle J_x^2 \rangle = 0$ , which also correspond to point D. For example, such a state is the multiparticle singlet. However, usual spin-squeezing procedures remain in the symmetric subspace, thus we discuss only the Dicke state.
- [66] Z. Zhao, Y.-A. Chen, A.-N. Zhang, T. Yang, H. J. Briegel, and J.-W. Pan, *Nature* **430**, 54 (2004).
- [67] Y.-F. Huang, B.-H. Liu, L. Peng, Y.-H. Li, L. Li, C.-F. Li, and G.-C. Guo, *Nat. Commun.* **2**, 546 (2011).
- [68] D. Leibfried, E. Knill, S. Seidelin, J. Britton, R. B. Blakestad, J. Chiaverini, D. B. Hume, W. M. Itano, J. D. Jost, C. Langer, R. Ozeri, R. Reichle, and D. J. Wineland, *Nature* **438**, 639 (2005).
- [69] G. Tóth, W. Wieczorek, D. Gross, R. Krischek, C. Schwemmer, and H. Weinfurter, *Phys. Rev. Lett.* **105**, 250403 (2010).
- [70] G. Tóth and I. Apellaniz, *J. Phys. A: Math. Theor.* **47**, 424006 (2014).
- [71] B. Escher, R. de Matos Filho, and L. Davidovich, *Nat. Phys.* **7**, 406 (2011); R. Demkowicz-Dobrzański, J. Kołodyński, and M. Guţă, *Nat. Commun.* **3**, 1063 (2012).
- [72] This is also relevant for Ref. [60], where  $\mathcal{F}_Q = O(N^2)$  is reached with weakly entangled states.
- [73] For some of the programs used for this article, see the actual version of the QUBIT4MATLAB package at <http://www.mathworks.com/matlabcentral/>. The 3.0 version of the package is described in G. Tóth, *Comput. Phys. Commun.* **179**, 430 (2008).
- [74] For MATLAB R2015a, see <http://www.mathworks.com>.